Hindawi
Scientific Programming
Volume 2022, Article ID 5299385, 10 pages
https://doi.org/10.1155/2022/5299385

Research Article

Magnetic Resonance Image under the Low-Rank Matrix Denoising Algorithm in Evaluating the Efficacy of Neoadjuvant Chemo-Radiotherapy for Rectal Cancer

Yulong Qi,[1,2] **Fei Feng**,[1] **Na Zhang**,[3] **Hui Zhang**,[1] **and Guanxun Cheng**[1,2]

[1]*Medical Imaging Center, Peking University Shenzhen Hospital, Shenzhen 518036, Guangdong, China*
[2]*Shantou University Medical College, Shantou 515041, Guangdong, China*
[3]*Shenzhen Institute of Advanced Technology, Chinese Academy of Sciences, Shenzhen 518055, Guangdong, China*

Correspondence should be addressed to Guanxun Cheng; 1400540231@xs.hnit.edu.cn

Received 6 October 2021; Accepted 21 February 2022; Published 23 March 2022

Academic Editor: M Pallikonda Rajasekaran

This study was to explore the application value of magnetic resonance imaging (MRI) images obtained by low-rank matrix recovery algorithm (LRMR algorithm) in evaluating the curative effect of rectal cancer patients receiving the neoadjuvant chemo-radiotherapy (nCRT). In this study, an image denoising model was designed based on the LRMR algorithm, the original low-rank data matrix was recovered from the error, and the low-rank matrix was restored by solving the optimal kernel norm, so as to effectively separate the image data information and the interference noise. In addition, the model was applied to 60 patients with rectal cancer who received nCRT to extract the texture parameters and lesion-related data from the MRI images. The results showed that the MRI images optimized by LRMR algorithm were clearer than the original images, contained less excess noise, and had improved imaging accuracy and image quality. The results of typical cases suggested that the front of the rectal wall membrane of a patient in the T-downstage group was not smooth before treatment, the internal angiography was blurred, and the wall membrane was thickened, but the wall membrane became thinner after treatment, the highest position was reduced from 1.46 cm to 0.38 cm, the average value of the apparent diffusion coefficient (ADC) increased from 0.732×10^{-3} mm^2/s to 1.196×10^{-3} mm^2/s, and the lesion tissue was thicker. It was found that the height, length, and ADC of the lesion after the nCRT showed statistically great difference in contrast to the values before the treatment ($P < 0.05$). Such results indicated that the nCRT showed obvious effects in the clinical treatment of rectal cancer. In short, the LRMR algorithm could remove the interference noise in the MRI image, and from the information about rectal cancer tumor lesions extracted from that, the height value and length value of tumor lesions in patients given neoadjuvant chemo-radiotherapy were reduced compared with those before treatment, and the apparent diffusion coefficient value was increased, indicating that neoadjuvant chemo-radiotherapy has a significant effect in the clinical treatment of rectal cancer.

1. Introduction

Rectal cancer refers to cancer that arises from the boundary between the rectum and anal canal to the junction of the sigmoid colon. It is a common malignant tumor of the digestive tract [1, 2]. The cause of rectal cancer is still unclear, and it is mostly related to the surrounding environment, eating habits, and genetic factors. The age of onset of rectal cancer in China is mostly around 45 years old, and there is a younger trend in recent years [3, 4]. Rectal cancer is generally diagnosed pathologically through digital examination and colonoscopy. However, it is located in the deep pelvic cavity with complex surrounding tissues. Under some other pathological reasons, the postoperative recurrence rate and metastasis rate are still very high [5]. Nowadays, neoadjuvant chemo-radiotherapy (nCRT) has gradually come into people's sight, and its advantages have been confirmed through repeated clinical practice. nCRT can inhibit the primary lesion, reduce its area significantly, control the proliferation and metastasis of tumor cells, and improve the

clinical symptoms of patients, so that the patients can receive better surgical treatment [6, 7].

In the early stage of rectal cancer, most of the patients show no obvious symptoms, so medical imaging has become an important clinical examination method. The first choice is magnetic resonance imaging (MRI). It is non-invasive, easy to operate, and multi-faceted imaging. In addition, it shows high resolution on soft tissue, can identify the location of the tumor, and display the structure between the tumor and adjacent tissues, which is helpful for doctors to judge the stage of the disease and adopt corresponding treatment methods [4, 8]. However, MRI medical images cannot guarantee the complete display rate due to the level of imaging equipment and other reasons, and it often shows uneven light exposure and redundant interference information, resulting in deviations in the information and data obtained, increasing unnecessary burden for doctors in clinical work [9].

With the development of science and technology, low-rank matrix recovery (LRMR) algorithm has become more and more widely used in our lives. It refers to automatically distinguishing some lost elements of a matrix and treating the degraded image as a set of low-dimensional data plus noise. Therefore, the data before degradation can be approximated by the LRMR algorithm to restore the original matrix, to achieve the data and noise division [10]. Applying this algorithm to MRI imaging technology can reduce the interference noise, enhance the display of image details, and improve the accuracy of detection, which is of great significance for evaluating the clinical curative effect of nCRT on rectal cancer [11].

The objective of this study was to apply the LRMR algorithm to MRI to extract the texture feature parameters in the obtained image, so as to analyze the clinical curative effect of nCRT on rectal cancer, providing a more accurate basis on how to choose the treatment of rectal cancer in clinic.

2. Materials and Methods

2.1. Research Objects. Sixty patients with rectal cancer at the hospital from August 2018 to October 2020 were selected as the research objects in this study. They all received nCRT and had undergone the total mesorectal excision (TME). There were 40 male cases and 20 female cases, aged 45–51 years old (with an average age of 48 years old). This experiment had been approved by the ethics committee of the hospital, and all experimental matters had been informed to the patient and his/her family members, who had signed the informed consent forms.

Inclusion criteria were as follows: patients who were pathologically diagnosed with rectal cancer; patients whose clinical tumor node metastasis (TNM) tumor staging was confirmed by MRI before nCRT; patients whose rectal cancer tumor staging was T3-4 (T3: larger and/or infiltration beyond the margin of primary organ; T4: very large and/or infiltration into adjacent organs) without distant metastasis; patients who received the TME after the nCRT; and patients with complete clinical data.

Exclusion criteria were as follows: patients who were pathologically diagnosed with mucinous adenocarcinoma; patients with familial polypoid adenoma; patients with previous history of other malignant tumors; patients with incomplete MRI imaging results for analysis; and patients with incomplete clinical data.

2.2. nCRT. The nCRT program in this study was performed with the linear accelerator 6MV-X-ray for traditional segmentation. The total pelvic radiotherapy radiation dose was 40–50 Gy (with 2 Gy once), the radiation had to be continued for successive 5 days a week, and the radiation was repeated after 2 days. The total number of exposures was 20–25 times, and the irradiation should be continued for 5 weeks. The nCRT program was defined as follows. From the day when the nCRT was started, the patient was required to take capecitabine tablets (1250 mg/m^2) orally with 2 times a day, which should be continued for 5 days without any suspension and then stopped for 2 days. A course of treatment should be one week, and the oral administration should be required for a total of 5 weeks till the nCRT was finished.

2.3. LRMR Algorithm. The concept of LRMR algorithm was to recover a data matrix with a lower rank from a slightly larger error but with a small number of non-zero elements in the matrix, which was deemed as the sum of the rank matrix and the noise matrix. Then, solving the optimal kernel norm was adopted to restore the low-rank matrix. It was supposed that in addition to the original information, the image data also included a part of noise, which meant that the original data were regarded as the sum of a low-rank matrix and a sparse matrix. For example, the low-rank matrix A was interfered by the sparse matrix O and converted to matrix B, so the low-rank matrix had to be restored firstly, as described below:

$$\begin{aligned} &\min\ \operatorname{rank}(A) + X\|O\|_0 \\ &\text{S.t}\ A + O = B. \end{aligned} \tag{1}$$

In the above equation, X was the decision function, rank(A) represented the rank of matrix A, and $\|O\|_0$ referred to the zero norm of matrix O. In the process of solving, it was found that rank(A) and $\|O\|_0$ were very computationally intensive, so the solution of norm minimization A_1 was infinitely close to the solution of norm minimization A_0. Then, (1) could be written as follows:

$$\begin{aligned} &\min\ \|A\|_0 + X\|O\|_1 \\ &\text{S.t.}\ A + O = B. \end{aligned} \tag{2}$$

In the above equation, $\|A\|_0$ was the kernel norm of the function, which represented the sum of the eigenvalues of all matrices. In the low-rank matrix theory, matrix B represented the image containing noise; A represented the original image that should be restored; and O referred to the lonely and scattered noise in the image. Therefore, under the precondition of without obtaining experience and historical

data, solving (2) could separate the noise from the image data with noise, restore the original image, and more completely preserve the corners, texture parameters, and other subtleties of the image.

After the denoising was completed, it was necessary to evaluate the effect, such as the smoothness and flatness of the image after denoising, whether the corners were clear enough, whether some detailed information was lost, and whether there was distortion compared with the original image. The mathematical evaluation method of this experiment was the peak signal-to-noise ratio method, which could determine the intelligibility and simulation degree of the image. The concept was described as follows:

$$\mathrm{PSNR} = 5 \log_5 \left[\frac{150^2}{(1/UV) \sum_{p=1}^{u} \sum_{t=1}^{v} \left(C_{pt} - D_{pt} \right)^2} \right]. \quad (3)$$

In the equation above, C_{pt} and D_{pt} represented the gray level of the denoised image and the original image, respectively, and U and V represented the row and column of the image, respectively. Peak signal-to-noise ratio (PSNR) was the image quality evaluation index. The higher the PSNR, the greater the denoising intensity of the algorithm.

2.4. MRI Examination. All patients had a low fiber diet 3 days before MRI, used drugs to clean their intestines within 12 hours before MRI, banned digital rectal examination, sigmoidoscopy and other examinations, and fasted within 6 hours before MRI. Before the examination, a medical coupling agent was injected into the anus to help clear the ultrasound image. All patients were examined with MRI machine and 16-channel body phased array coil of the same brand. The MRI scan sequence included the axial T1-weighted imaging (T1WI) sequence, oblique axial high-resolution T2-weighted imaging (T2WI) sequence perpendicular to the lesion, sagittal T2WI sequence, and oblique coronal T2WI sequence parallel to the lesion.

2.5. Image Analysis. The full quantitative postprocessing Matlab software was adopted to extract the texture feature parameters in the MRI image after denoising by the LRMR algorithm, and a professional imaging doctor with rich experience in rectal MRI diagnosis was required to check the MRI images of all the examined patients. The part with the largest rectal tumor area was selected for image analysis, and the relevant data were recorded for subsequent use. Before image segmentation, all the original images were standardized and calibrated firstly, and then two professional doctors with rich experience in gastrointestinal imaging diagnoses were required to select the largest rectal tumor area without being informed of any clinical data of the patient. Image segmentation was performed on a part of the image, and the relevant texture feature parameters were collected. The length value, height value, and the average apparent diffusion coefficient (ADC) of all patients before and after nCRT treatment were measured for the largest tumor area.

According to the 7th edition of the staging system standards issued by the American Cancer Federation and the International Anti-Cancer Alliance, the imaging stage diagnosed by the MRI image was selected as the primary tumor condition of patients before the nCRT, which referred to the T stage. Based on the final pathological stage after the completion of the nCRT, patients can be rolled into two groups: T-downstage group and T-non-downstage group. The ADC, length, and height of all rectal cancer patients were measured before and after nCRT for comparisons. All patients in the T-downstage group and T-non-downstage group were tested for differences in their tumor ADC, length, and height values before the nCRT was given. In addition, the ADC difference, length difference, height difference, ADC change rate, length change rate, and height change rate of patients in the T-downstage group and T-non-downstage group were observed and compared before and after the nCRT. All the data in this experiment were automatically calculated by computer software.

2.6. Follow-Up Visit. The patients received follow-up visit by telephones. Every surviving patient had to be followed up for at least 5 years after TME at the frequency of every 3 months within the first year after surgery, every half an hour in the second and third year, and every other year in the 4th and 5th years.

In the survival analysis of this experiment, the characteristic events that reflect the failure or ineffectiveness of treatment measures were manifested as disease development, such as tumor recurrence, distant metastasis, or the final death of the patient due to various factors. The criterion referred to the disease-free survival, which was the time from randomization to disease recurrence or patient death due to disease progression. For patients who were lost to follow-up due to incorrect phone calls, shutdowns, disconnection, and refusal to follow-up, their disease-free survival ranged from the first day after TME to the last follow-up before loss to follow-up. For patients with no failure events, the disease-free survival period ranged from the first day after TME to the day when the experiment ceased follow-up. These data were marked as truncated data, and the follow-up information of all other valid patients was fully included in the database.

2.7. Statistical Analysis. The SPSS 24.0 software was used for statistical analysis, and the Kolmogorov–Smirnov test was adopted to analyze whether the experimental data were consistent with the Gaussian distribution. If it did, the t test was used. $P < 0.05$ meant that the difference was statistically significant. The ADC, length, and height of all rectal cancer patients before and after nCRT, the tumor ADC, length, and height values before the nCRT of patients in the T-downstage group and T-non-downstage group and the ADC difference, length difference, height difference, ADC change rate, length change rate, and height change rate of patients in the T-downstage group and T-non-downstage group were performed with the test of normality. If the Gaussian distribution was met, the t test was selected. $P < 0.05$ meant that

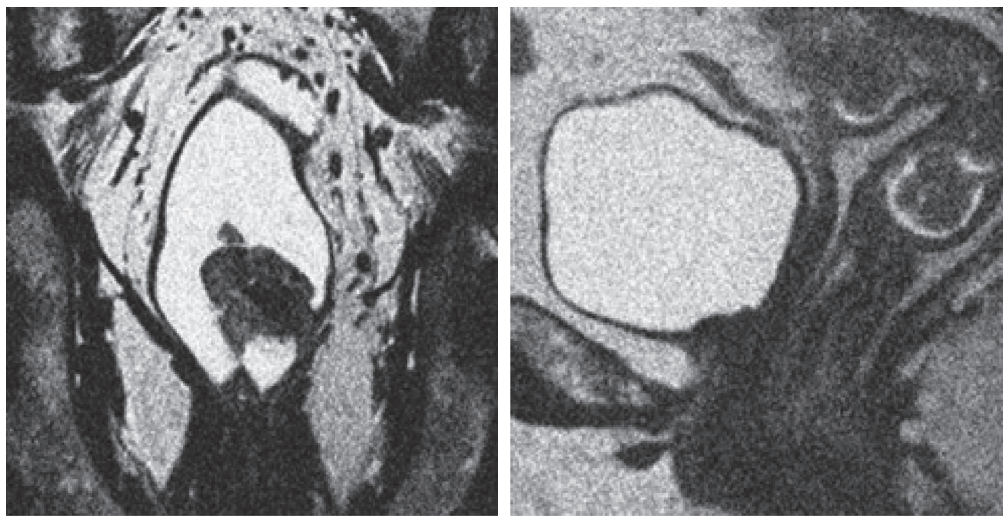

Figure 1: Original MRI images of a male patient.

the difference showed statistical significance. The Wilcoxon signed rank test was applied to compare the differences in texture parameters before and during the nCRT. The Mann–Whitney rank sum test was adopted to evaluate the differences in texture parameters between groups with different curative effects. $P < 0.05$ indicated that the difference was statistically significant.

3. Results

3.1. Comparative Analysis of MRI Images before and after Using the LRMR Algorithm. A patient in the T-downstage group, male, 50 years old, received the routine MRI examination before the nCRT. However, the MRI image was unclear and there was extra interference noise (Figure 1) due to the lower level of imaging equipment, which made it difficult to observe the details of the tumor in the intestinal wall. Therefore, the LRMR algorithm was applied in MRI imaging technology, and the image obtained was clear without unnecessary noise, as shown in Figure 2.

3.2. Number of T Stage of Rectal Cancer Patients before and after Receiving nCRT. Before nCRT treatment, there were 35 patients with T3 stage and 25 patients with T4 stage. After the nCRT, there were 17 patients with T1 staging, 10 with T2 staging, 28 with T3 staging, and 5 with T4 staging, as shown in Figure 3.

3.3. Consistency of MRI Image Texture Parameters in Patients with Rectal Cancer. Before and after the nCRT, two professional physicians with rich experience in gastrointestinal imaging diagnosis used the LRMR algorithm to extract clear relevant texture feature parameters from the selected MRI images of the largest level of rectal tumors, and the range of correlation coefficient values within the group was 0.73–0.99, showing good consistency and reliability (as given in Figure 4).

3.4. Comparison of the Tumor Height, Length, and ADC in Patients with Rectal Cancer before and after nCRT. The tumor height, length, and ADC in the MRI images obtained through the LRMR algorithm were compared for all patients with rectal cancer before and after the nCRT was given, and the results are illustrated in Figure 5. It showed that the tumor height and length values after nCRT were smaller than those before the nCRT, but the ADC value of the tumor was much higher, showing statistically obvious differences ($P < 0.05$).

3.5. Comparison of Tumor Height, Length, and ADC for Patients between T-Downstage Group and T-Non-Downstage Group before nCRT. All rectal cancer patients were rolled into a T-downstage group and a T-non-downstage group, and the maximum height value, length value, and ADC in the MRI images obtained by the LRMR algorithm were compared for patients in the two groups before the nCRT was given. As illustrated in Figure 6, the results showed no statistical significance ($P > 0.05$).

3.6. Comparison of MRI Image Texture Parameters for Patients between the T-Downstage Group and T-Non-Downstage Group. All rectal cancer patients were rolled into a T-downstage group and a T-non-downstage group. The texture parameters of MRI images based on LRMR algorithm were analyzed and compared, including the standard deviation value, homogeneity, energy, and entropy before nCRT as well as the average and entropy during the nCRT. The results showed statistically observable difference ($P < 0.05$), as given in Figures 7 and 8.

3.7. Comparison of Height Difference, Length Difference, and ADC Difference of Tumor in Patients between the T-Downstage Group and T-Non-Downstage Group before and after nCRT. The height difference and length difference of tumor in the MRI images obtained using the LRMR algorithm showed no statistical differences between the T-downstage group and

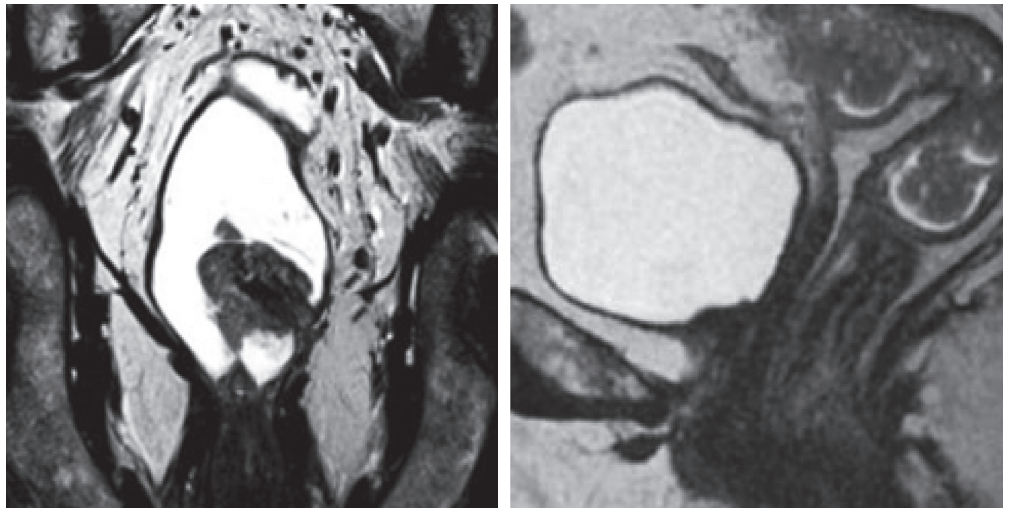

Figure 2: The MRI images after processing with the LRMR algorithm.

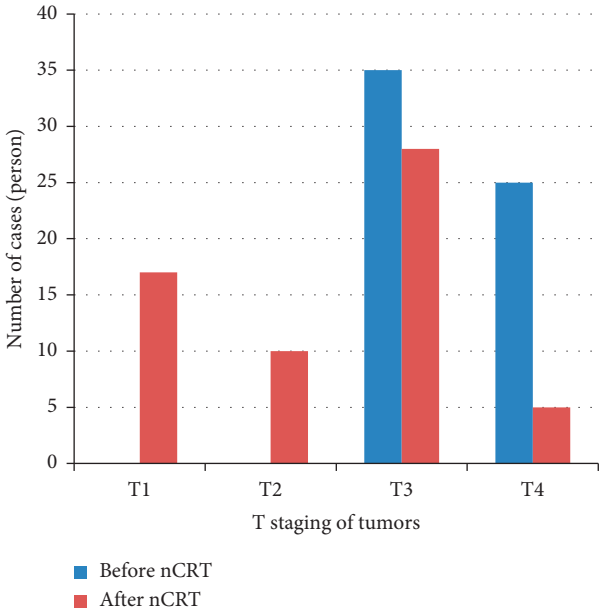

Figure 3: Number of cases in different T stage of rectal cancer before and after nCRT treatment.

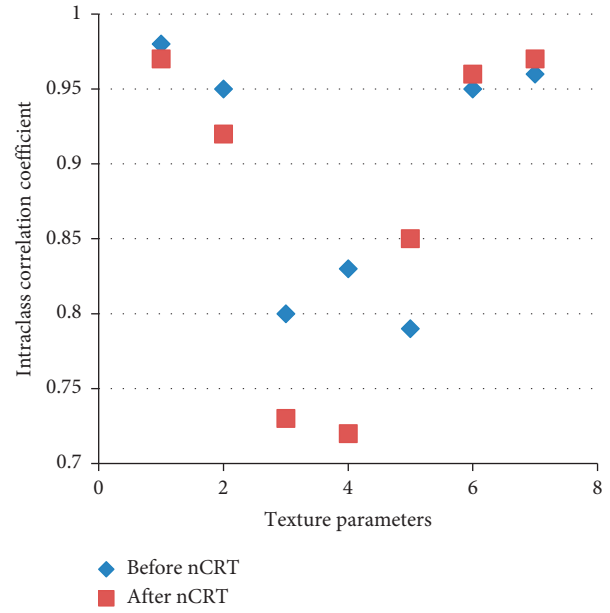

Figure 4: Consistency of MRI image texture parameters before and after nCRT. 1, 2, 3, 4, 5, 6, and 7 represented the average, the standard deviation, the skewness coefficient, the kurtosis coefficient, the homogeneity, energy, and the entropy value, respectively.

T-non-downstage group before and after the nCRT ($P > 0.05$), while the ADC difference showed statistical difference ($P < 0.05$), as shown in Figure 9.

3.8. Comparison of Height Change Rate, Length Change Rate, and ADC Change Rate of Tumor in Patients between T-Downstage Group and T-Non-Downstage Group before and after nCRT. All rectal cancer patients were divided into a T-downstage group and a T-non-downstage group. The height change rate and length change rate of the tumor in the MRI images obtained by the LRMR algorithm before and after the nCRT were compared between the two groups, and the results suggested that the differences were not statistically significant ($P > 0.05$), while the ADC change rate was statistically different ($P < 0.05$), as shown in Figure 10.

3.9. Case Analysis

Case 1. A patient in the T-downstage group, male, 50 years old, suffered from an intermittent discharge of pus and blood for 2 months. After nCRT was given, the lesion tissue in the rectum of the patient was thinner, and the ADC value was greatly higher than that before nCRT, as shown in Figures 11 and 12.

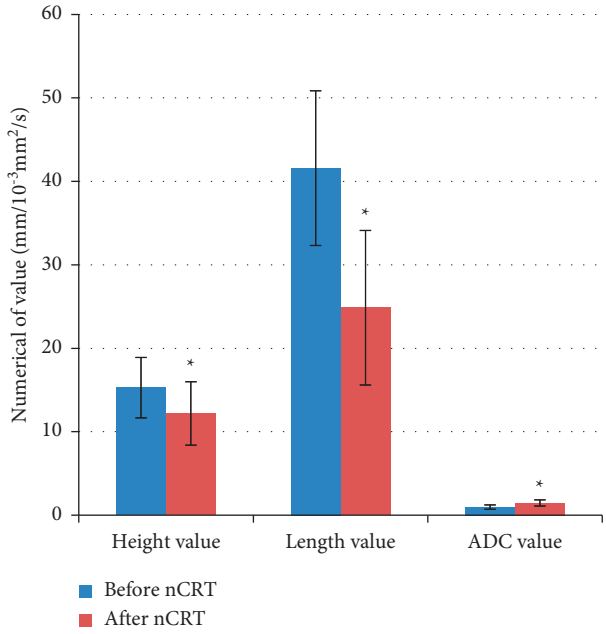

Figure 5: Comparison of tumor height, length, and ADC in patients with rectal cancer before and after nCRT. *indicated that the height value, length value, and ADC of the tumor after nCRT were statistically different from those before nCRT ($P < 0.05$).

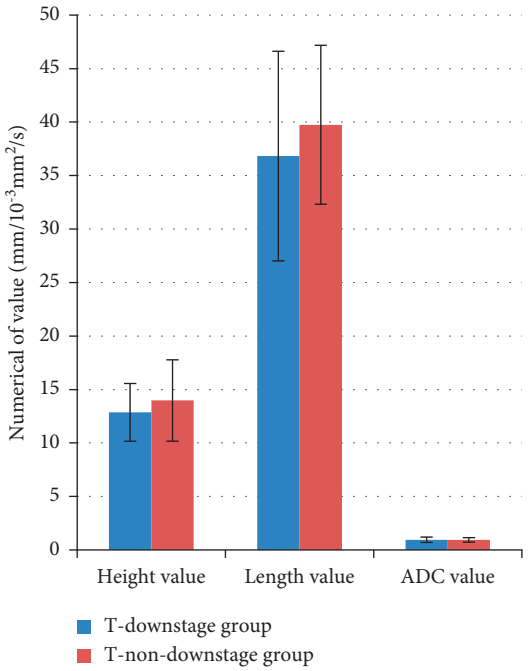

Figure 6: Comparison of tumor height, length, and ADC for patients between T-downstage group and T-non-downstage group before nCRT.

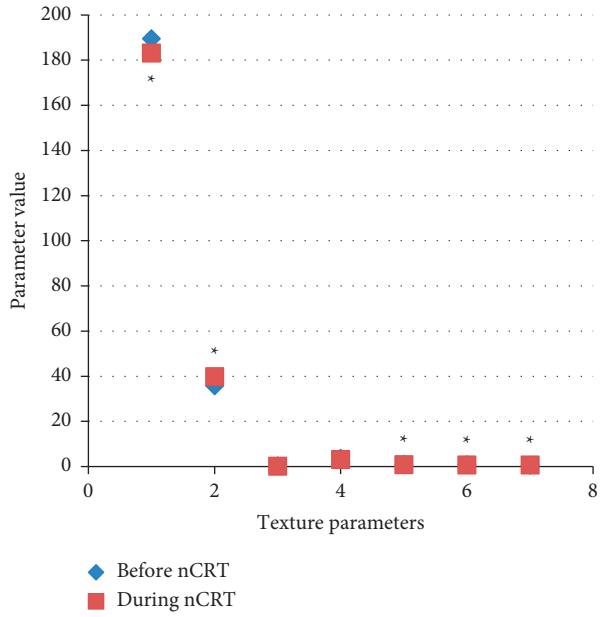

Figure 7: Comparison of MRI image texture parameters of T-downstage group before and during the nCRT. 1, 2, 3, 4, 5, 6, and 7 represented the average, the standard deviation, the skewness coefficient, the kurtosis coefficient, the homogeneity, energy, and the entropy value, respectively. *indicated that the texture parameters (1, 2, 5, 6, and 7) in the T-downstage group before nCRT were statistically different from those during the nCRT ($P < 0.05$).

Case 2. A patient with rectal cancer in the T-non-downstage group, female, 47 years old, suffered from intermittent diarrhea, pus, and bloody stool for more than 3 months. After nCRT was given, the MRI image based on the LRMR algorithm showed that the tumor lesions in the rectum did not change from thick to thin, and its ADC value decreased slightly compared with the previous one, as shown in Figures 13 and 14.

4. Discussion

Rectal cancer is a kind of cancer formed by malignant transformation of rectal tissue cells, and it is one of the most common gastrointestinal cancers in the world. Rectal cancer

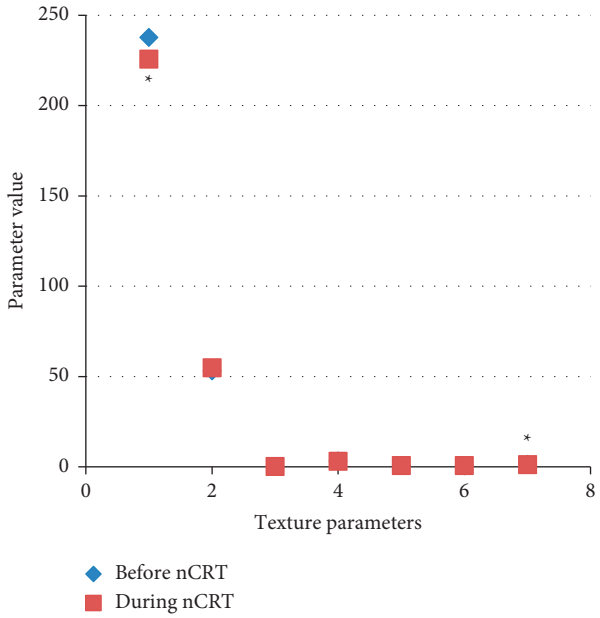

Figure 8: Comparison of MRI image texture parameters of T-non-downstage group before and during nCRT. 1, 2, 3, 4, 5, 6, and 7 represented the average, the standard deviation, the skewness coefficient, the kurtosis coefficient, the homogeneity, energy, and the entropy value, respectively. *suggested that the difference in texture parameters (1 and 7) in the T-non-downstage group before nCRT was statistically different from that during the nCRT ($P < 0.05$).

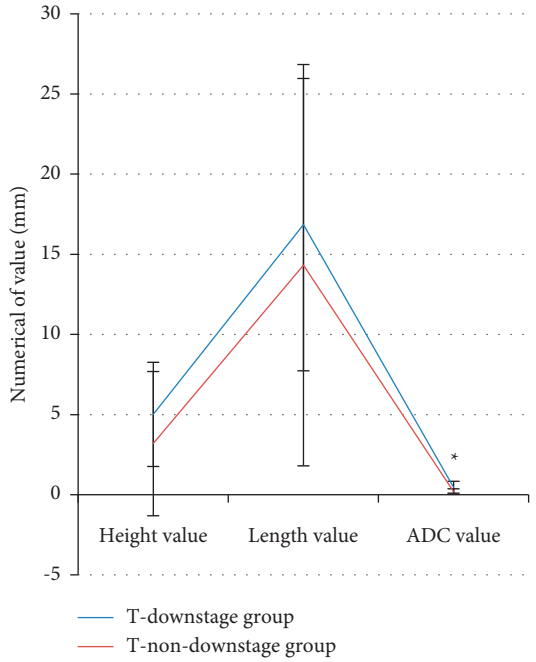

Figure 9: Comparison of height difference, length difference, and ADC difference of tumor in patients between the T-downstage group and T-non-downstage group before and after nCRT. *represented that the ADC difference of tumors in the T-downstage group and the T-non-downstage group after nCRT was statistically different from that before nCRT ($P < 0.05$).

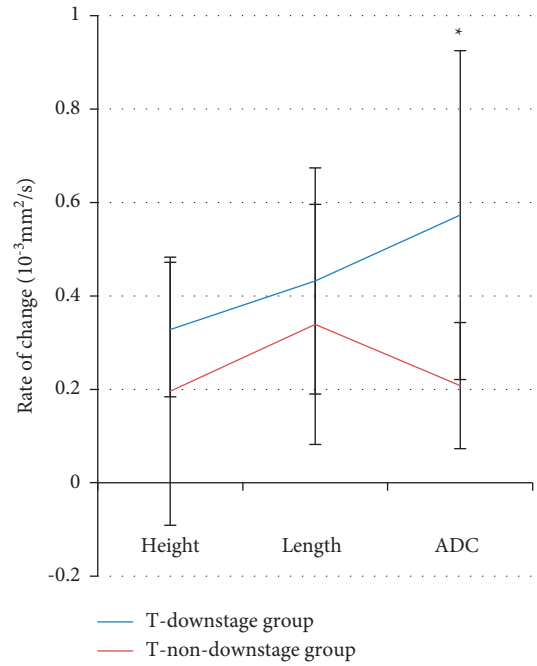

Figure 10: Comparison of height change rate, length change rate, and ADC change rate of tumor in patients between T-downstage group and T-non-downstage group before and after nCRT. *represented that the ADC change rate of tumors in the T-downstage group and the T-non-downstage group after nCRT was statistically different from that before nCRT ($P < 0.05$).

shows basically no obvious symptoms in the early stage, and most of the patients are in the middle and late stages when they are diagnosed. The onset of rectal cancer is hidden, its location in the pelvic cavity is complicated, the surgery is difficult, and the recurrence and metastasis rate is high after the middle and late stages, which seriously reduces the quality of life of the patients [12, 13]. Nowadays, nCRT has become a universally effective treatment method, and it is used more and more widely in clinical practice. For the early diagnosis of rectal cancer, medical imaging is an important clinical examination method. Among them, MRI technology is the first choice. However, MRI images may show uneven illumination and noise due to factors such as imaging equipment, which prevents the readers from being able to diagnose the disease, bringing some trouble for accurate judgments in clinic [14]. Therefore, the LRMR algorithm was applied to MRI images in this study, which could remove the noise, display clearly, and improve the accuracy of imaging [15].

In this study, 60 patients with rectal cancer were selected, and the texture parameters related to the rectal tumor in the MRI image were extracted through the LRMR algorithm. In addition, the height, length, and ADC values of tumor of all patients were compared before and after nCRT. The results revealed that in patients who were given nCRT, the differences in the height, length, and ADC maximum of tumor lesions were statistically observable ($P < 0.05$). Such results indicated that nCRT reduced the height and length of tumor lesions. The increased ADC indicated that nCRT had a

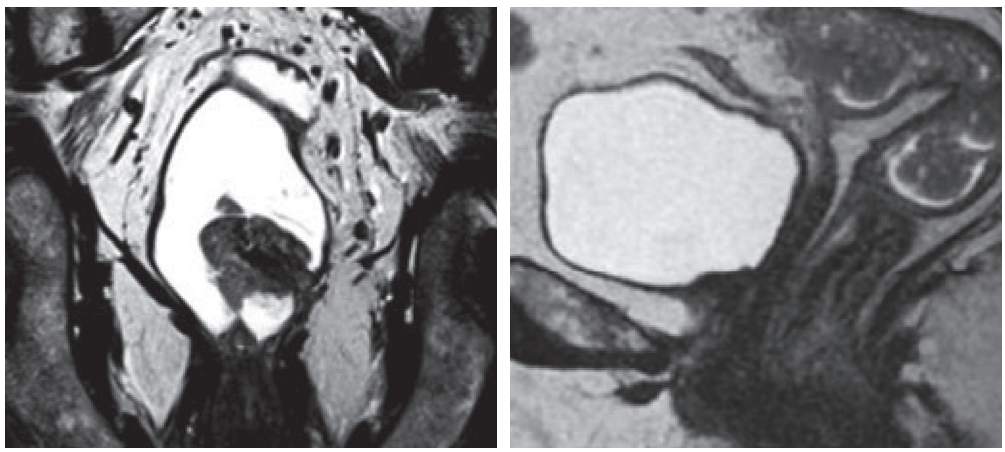

Figure 11: Before nCRT treatment, the MRI image based on the LRMR algorithm showed that the oblique-axis high-resolution T2-weighted imaging sequence showed that the front of the rectal wall was not smooth, the internal rectal radiography was blurred, and the wall was thickened, which was 1.46 cm maximal. The axial ADC showed that the ADC was about 0.732×10^{-3} mm^2/s.

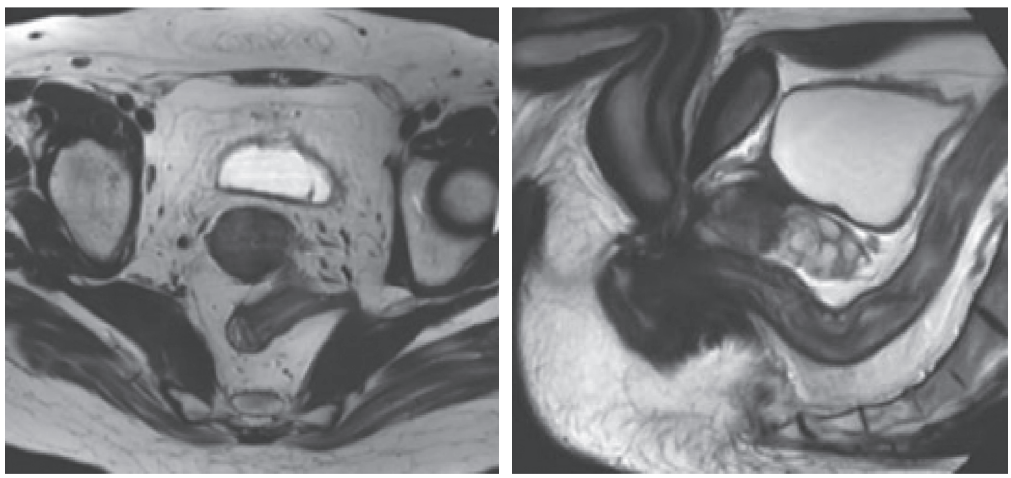

Figure 12: After treated with nCRT, the patient underwent MRI again. The MRI images based on the LRMR algorithm showed that the high-resolution oblique-axis T2-weighted imaging showed that the rectal wall was thinner than before nCRT, and the highest position was about 0.38 cm. The axial ADC showed that the average ADC was 1.196×10^{-3} mm^2/s, which was much higher in contrast to the value before nCRT.

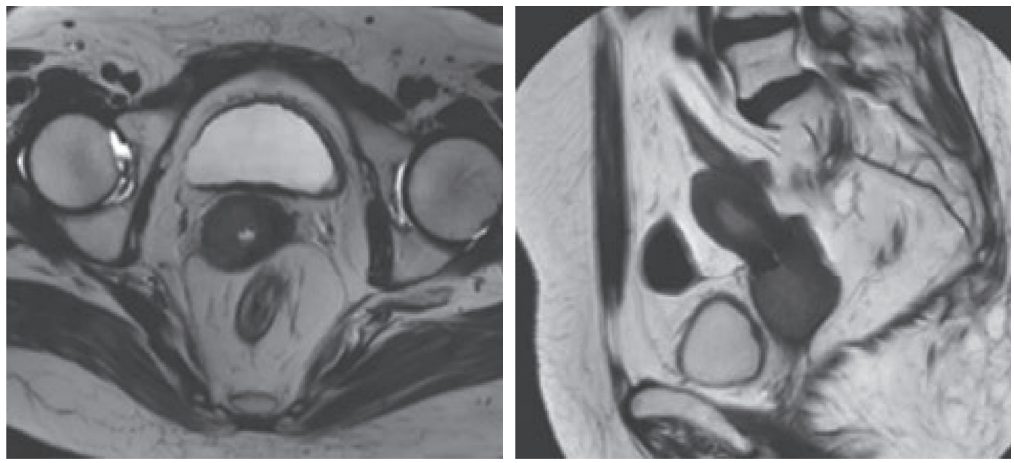

Figure 13: The patient received MRI examination before nCRT, and the results based on the LRMR algorithm showed that the oblique-axis high-resolution T2-weighted imaging showed that the front of the rectal wall was not smooth and uneven, and the wall was thickened, the highest was about 1.7 cm, and the cancer cell lesions diffused throughout the layer. The axial ADC showed that the average ADC was 1.278×10^{-3} mm^2/s.

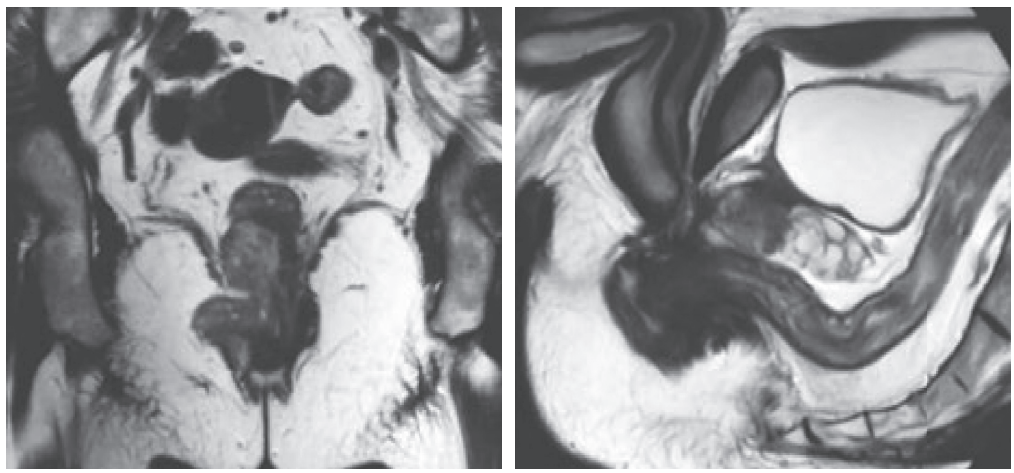

Figure 14: The patient underwent MRI again after receiving nCRT, and the MRI image based on the LRMR algorithm showed that the oblique-axis high-resolution T2-weighted imaging showed that the thickness of the rectal tumor lesion was not greatly different from the previous one, the highest position was about 1.75 cm, the cancerous lesions were diffused throughout the entire thickness, and the edges were blurred. The axial ADC showed that the average ADC value was 1.126×10^{-3} mm^2/s, which was lower than that before nCRT.

definite curative effect in the clinical treatment of rectal cancer [16]. The experimental results were in line with expectations because a number of previous studies showed that the denoising model constructed by low-rank matrix algorithm has a positive role in noisy MRI images and can decompose and extract noise so as to achieve the purpose of optimizing images. In 2019, Mao et al. put forward the theory of LRMR algorithm in an article to perform low-rank decomposition of approximate blocks, which could effectively segment the image data information and noise, thereby removing the excess noise in the image [17]. Dayde et al. [18] also reported that nCRT had good preoperative tissue oxygenation and good therapeutic efficacy, while avoiding the radiation proctitis of postoperative radiotherapy caused by postoperative surgical field adhesion and fixation, and the difficulty of surgery and the incidence rate of complications were also reduced. The reliability of these statements were confirmed in this study. A low-rank matrix algorithm was used to build a model to decompose and extract the noisy MRI images and compare the texture feature parameters in the obtained images and the relevant values of tumor lesions before and after the treatment [19], so as to analyze the clinical curative effect of nCRT on rectal cancer, which played an important role in the clinical treatment of rectal cancer.

5. Conclusion

An image denoising model was constructed based on the LRMR algorithm and applied to the MRI images of 60 patients with rectal cancer who received nCRT in this study. It was found that the MRI image after denoising by the LRMR algorithm was clearer than the ordinary MRI image, and the display of image details was enhanced. From the information extracted from it on rectal cancer tumor lesions, neoadjuvant chemo-radiotherapy has a significant effect in the clinical treatment of rectal cancer. However, the number of patient samples was small and the source was single. For the two MRI examinations before and after nCRT, the selected ranges for analysis may not all be the same, and the application of LRMR algorithm in MRI image information was not universal enough. In addition, it lacked deeper analysis and discussion. It is believed that LRMR algorithm would play a greater role in the medical field with the development of technology.

Data Availability

The data used to support the findings of this study are available from the corresponding author upon request.

Conflicts of Interest

The authors declare that they have no conflicts of interest.

References

[1] N. Wilkinson, "Management of rectal cancer," *Surgical Clinics of North America*, vol. 100, no. 3, pp. 615–628, 2020 Jun.

[2] E. B. Ludmir, M. Palta, C. G. Willett, and B. G. Czito, "Total neoadjuvant therapy for rectal cancer: an emerging option," *Cancer*, vol. 123, no. 9, pp. 1497–1506, 2017.

[3] G. Feeney, R. Sehgal, M. Sheehan et al., "Neoadjuvant radiotherapy for rectal cancer management," *World Journal of Gastroenterology*, vol. 25, no. 33, pp. 4850–4869, 2019.

[4] N. Horvat, C. Carlos Tavares Rocha, B. Clemente Oliveira, I. Petkovska, and M. J. Gollub, "MRI of rectal cancer: tumor staging, imaging techniques, and management," *Radio-Graphics*, vol. 39, no. 2, pp. 367–387, 2019.

[5] Y.-L. Hsu, C.-C. Lin, J.-K. Jiang et al., "Clinicopathological and molecular differences in colorectal cancer according to location," *The International Journal of Biological Markers*, vol. 34, no. 1, pp. 47–53, 2019.

[6] L. Brandariz, M. Arriba, J. L. García et al., "Differential clinicopathological and molecular features within late-onset colorectal cancer according to tumor location," *Oncotarget*, vol. 9, no. 20, pp. 15302–15311, 2018.

[7] T. Higaki, Y. Nakamura, F. Tatsugami, T. Nakaura, and K. Awai, "Improvement of image quality at CT and MRI using deep learning," *Japanese Journal of Radiology*, vol. 37, no. 1, pp. 73–80, 2019.

[8] X. Jia, X. Feng, W. Wang, and L. Zhang, "Generalized unitarily invariant gauge regularization for fast low-rank matrix recovery," *IEEE Transactions on Neural Networks and Learning Systems*, vol. 32, no. 4, pp. 1627–1641, 2021.

[9] R. G. H. Beets-Tan, D. M. J. Lambregts, M. Maas et al., "Magnetic resonance imaging for clinical management of rectal cancer: updated recommendations from the 2016 European Society of Gastrointestinal and Abdominal Radiology (ESGAR) consensus meeting," *European Radiology*, vol. 28, no. 4, pp. 1465–1475, 2018.

[10] B. Gürses, M. Böge, E. Altınmakas, and E. Balık, "Multiparametric MRI in rectal cancer," *Diagnostic and Interventional Radiology*, vol. 25, no. 3, pp. 175–182, 2019.

[11] F. Monni, P. Fontanella, A. Grasso et al., "Magnetic resonance imaging in prostate cancer detection and management: a systematic review," *Minerva Urology and Nephrology*, vol. 69, no. 6, pp. 567–578, 2017.

[12] J. Hou, F. Zhang, H. Qiu, J. Wang, Y. Wang, and D. Meng, "Robust low-tubal-rank tensor recovery from binary measurements," *IEEE Transactions on Pattern Analysis and Machine Intelligence*, 2021.

[13] T. Draeger, V. Völkel, M. Gerken, M. Klinkhammer-Schalke, and A. Fürst, "Long-term oncologic outcomes after laparoscopic versus open rectal cancer resection: a high-quality population-based analysis in a Southern German district," *Surgical Endoscopy*, vol. 32, no. 10, pp. 4096–4104, 2018.

[14] R. E. Gabr, G. B. Zunta-Soares, J. C. Soares, and P. A. Narayana, "MRI acoustic noise-modulated computer animations for patient distraction and entertainment with application in pediatric psychiatric patients," *Magnetic Resonance Imaging*, vol. 61, pp. 16–19, 2019.

[15] R. J. M. Navest, S. Mandija, T. Bruijnen et al., "The noise navigator: a surrogate for respiratory-correlated 4D-MRI for motion characterization in radiotherapy," *Physics in Medicine and Biology*, vol. 65, no. 1, 2020.

[16] A. Qin, L. Xian, Y. Yang, T. Zhang, and Y. Y. Tang, "Low-rank matrix recovery from noise via an MDL framework-based atomic norm," *Sensors*, vol. 20, no. 21, p. 6111, 2020.

[17] Y. Mao, L. Han, and Z. Yin, "Cell mitosis event analysis in phase contrast microscopy images using deep learning," *Medical Image Analysis*, vol. 57, pp. 32–43, 2019.

[18] D. Dayde, I. Tanaka, R. Jain, M. Tai, and A. Taguchi, "Predictive and prognostic molecular biomarkers for response to neoadjuvant chemoradiation in rectal cancer," *International Journal of Molecular Sciences*, vol. 18, no. 3, p. 573, 2017.

[19] H. Chen, M. Wei, Y. Sun, X. Xie, and J. Wang, "Multi-patch collaborative point cloud denoising via low-rank recovery with graph constraint," *IEEE Transactions on Visualization and Computer Graphics*, vol. 26, no. 11, pp. 3255–3270, 2020.